PHYSICAL REVIEW B VOLUME 27, NUMBER 6 15 MARCH 1983

Atomic geometry of GaSb(110): Determination via elastic low-energy electron diffraction intensity analysis

C. B. Duke and A. Paton
Xerox Webster Research Center, Xerox Square-W114, Rochester, New York 14644

A. Kahn
Department of Electrical Engineering and Computer Science, Princeton University, Princeton, New Jersey 08544
(Received 3 November 1982)

Elastic low-energy electron diffraction (ELEED) intensities from GaSb(110) of normally incident electrons with energies $30 \leq E \leq 210$ eV were measured at $T=125$ K. Intensity versus incident-energy profiles were recorded for 14 diffracted beams. The surfaces were prepared by a chemical-polish—ion-bombard—anneal cycle. The stoichiometry of the surfaces and reproducibility of the data from one sample to another were verified explicitly. Comparison of these measured intensities with dynamical ELEED intensity calculations indicates that the dimensions of the surface unit cell are identical to those of truncated bulk GaSb, but that the atomic geometry within that cell is reconstructed. The best-fit structure consists of a bond-length—conserving rotation by $\omega_1=(30\pm2)°$ of species in the uppermost atomic layer with the Sb relaxing outward and the Ga inward. No displacements of the second-layer species are indicated by the analysis. The structure resembles those of ZnTe(110) and GaP(110), but is quite distinct from those of GaAs(110), InSb(110), and CdTe(110). This result reveals that ionicity alone is an inadequate index of the surface atomic geometries of compound semiconductors, independent of the definition chosen for the ionicity.

I. INTRODUCTION

For nearly two decades the establishment of relationships between interface properties and the nature of interface chemical bonds has been a major and controversial topic in studies of semiconductor interfaces.[1–5] Although for molecules and bulk solids the traditional means for establishing such relationships is via comparisons of atomic geometries with various indices of the nature of the chemical bond,[6–8] for interfaces a dearth of structural information has led to proposals of such relationships on the basis of comparisons of interface electrical properties with various indices of the strength of the bonds involved.[1–5] During the past five years, however, analyses of elastic low-energy electron diffraction (ELEED) intensities from the (110) (i.e., cleavage) surfaces of zinc-blende structure compound semiconductors have begun to provide a comprehensive view[9] of the richness of surface structures evident on these homologous surfaces of materials whose bulk structures are identical[10] and whose bonding is nominally "covalent."[7,8] Our purposes in this paper are to present and document our determination of the surface structure of GaSb(110) by ELEED intensity analysis and to comment upon the unique role which this structure plays in revealing the richness of semiconductor surface (as opposed to bulk) atomic geometries.

The definitions of the quantities specifying the atomic geometry of GaSb(110) are given in Fig. 1 in which the bulk structural parameters reported in Wyckoff[10] are utilized for the dimensions of the surface unit cell. Our main result is that GaSb is characterized by a bond-length—conserving rotation of $\omega_1=(30\pm2°)$ in the top layer and no further reconstruction of either the top or deeper layers. The structure is most reminiscent of those reported for ZnS(110) (Ref. 11) and GaP(110),[12,13] although in both of the latter cases the rotated top layer also is concentrated toward the substrate by 0.1 ± 0.05 Å. The relaxations of the Ga and Sb species normal to the surface (inward by 0.55 ± 0.05 Å and outward by 0.22 ± 0.05 Å, respectively) are essentially identical to those obtained earlier for the (110) surface of the isoelectric II-VI compound, ZnTe.[14] In contrast to GaSb, however, the relaxation parallel to the surface of the Te species in ZnTe was found to be reduced relative to that characteristic of a bond-length—conserving reconstruction: a result which could be caused either by a difference in bonding between II-VI and III-V compounds[15] or by the use of an older technology (nonrelativistic Slater exchange)

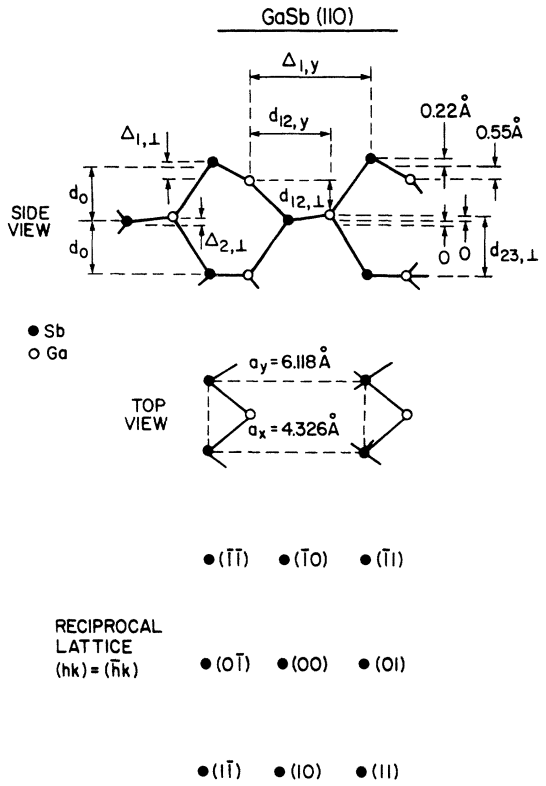

FIG. 1. Schematic indication of the surface atomic geometry and the associated ELEED normal incidence spot pattern for the (110) surface GaSb. The symbols utilized in Table I are defined in the upper panel of the figure. The numerical values shown are taken from panel (b) of Table I. The surface unit-cell parameters are those given by Wyckoff (Ref. 10).

to determine the structure of ZnTe.[16] A detailed discussion of the structural chemistry of GaSb(110) relative to the (110) surfaces of other zinc-blende structure compound semiconductors is given below.

We proceed by indicating the experimental procedures in Sec. II and defining our calculations in Sec. III. We present our structure analysis in Sec. IV and conclude with a discussion of our results.

II. EXPERIMENTAL PROCEDURES

The measurements of the ELEED intensities from GaSb(110) were performed in a standard Physical Electronics ultra-high-vacuum (UHV) LEED/Auger chamber equipped with a 4-grid Varian LEED (low-energy electron diffraction) optics and a single pass 4 kV Physical Electronics cylindrical mirror analyzer. The ELEED measurements were performed at a pressure of 1×10^{-10} Torr.

The sample was mechanically polished with 5 μm SiC powder and chemically etched in a 0.5% solution of bromine in methanol. The crystal was then mounted in a Mo foil and placed on a UHV sample manipulator allowing cooling to about 125 K. A Chromel-Alumel thermocouple, welded on the Mo foil, was used to measure the temperature. The surface was cleaned by Ar^+ ion sputtering (1.5 keV, grazing incidence) and the cleanliness of the surface was checked with Auger electron spectroscopy (AES). The sample was then annealed at about 430°C for 1 h to restore atomic order. A sharp (1×1) LEED pattern which exhibited the $(hk)=(\bar{h}k)$ symmetries observed on other (110) zinc-blende faces, resulted from this cleaning-annealing cycle. The sample was then cooled to 100 K, to reduce thermal atomic vibrations which, at room temperature, limit the intensity measurements to energies below 170 eV. The ELEED intensity data were recorded from the phosphor screen with a Gamma Scientific spot photometer and normalized to the incident beam current. Two sets of low-temperature (125 K) data were recorded at 2 V increments in primary beam voltage. The two sets of data were averaged in order to increase the signal-to-noise ratio. Each set included 14 beams, i.e., those with the beam indices (10) $=(\bar{1}0)$, (01), (0$\bar{1}$), (11) $=(\bar{1}1)$, (1$\bar{1}$) $=(\bar{1}\,1)$, (02), (0$\bar{2}$), (20) $=(\bar{2}0)$, (12) $=(\bar{1}2)$, (1$\bar{2}$) $=(\bar{1}\bar{2})$, (21), (2$\bar{1}$) $=(\bar{2}1)$, (13) $=(\bar{1}3)$, and (1$\bar{3}$) $=(\bar{1}\bar{3})$. Seven of these beams, the (10), (01), (0$\bar{1}$), (11), (1$\bar{1}$), (02), and (0$\bar{2}$) are much more intense then the rest. The (12) and (1$\bar{2}$) beams are of medium intensity, whereas the (20), (21), (2$\bar{1}$), (13), and (1$\bar{3}$) beams are weak.

III. MODEL CALCULATIONS

An approximate multiple-scattering model of the diffraction processes described previously[17] was used to perform our dynamical calculations of the ELEED intensities. In this model, which is embodied in a series of computer programs, the scattering species are represented by energy-dependent phase shifts in terms of which the ELEED intensities from the surface are computed. The scattering amplitudes associated with the uppermost three atomic bilayers are evaluated exactly, as are those of each of the individual atomic layers beneath. These amplitudes are superposed, weighted by appropriate phase factors, to obtain the diffracted intensities. The accuracy of this approximation has been verified in the analysis of other zinc-blende (110) surfaces, i.e., GaAs(110) and ZnTe(110), for which the intensity profiles calculated solving the scattering in the uppermost four atomic bilayers exactly were compared with those calculated solving the scattering in the uppermost three bilayers exactly. Convergence tests revealed that the consideration of a slab of six atomic layers and the use of six phase shifts for each

scatterer yield predicted intensities which are generally accurate to within a few percent, so these parameters were adopted for the calculations presented herein.

The electron-ion-core interaction is described by a one-electron muffin-tin (MT) potential. The one-electron crystal potential is formed from a superposition of overlapping ionic (e.g., Ga^+Sb^-) relativistic charge densities. These charge densities are obtained via self-consistent solutions to the Dirac equation for the individual ionic species. Given the charge densities, the phase shifts are evaluated by solving the nonrelativistic Schrödinger equation using the (energy-dependent) Hara model for the exchange potential.[16] A MT approximation to the crystal potential is imposed prior to the calculation of the phase shifts. The MT radii are taken to be the values at which the potentials of the Ga^+ and Sb^- cross, and the potential outside the muffin-tin spheres is taken to be the calculated value at the crossover point. Because the exchange potential depends on the energy of the incident electron, the crossover point and hence, the *MT* radii and crossover potentials also depend on this energy. Values of the radii range from $r_{MT}(Ga^+)=1.16$ Å and $r_{MT}(Sb^-)=1.48$ Å at an incident beam energy of $E=10$ eV, to $r_{MT}(Ga^+)=1.18$ Å and $r_{MT}(Sb^-)=1.46$ Å at $E=300$ eV. Values of the muffin-tin potential range from 12.7 eV at $E=10$ eV to 11.3 eV at $E=300$ eV. The phase shifts associated with these potentials are shown in Fig. 2.

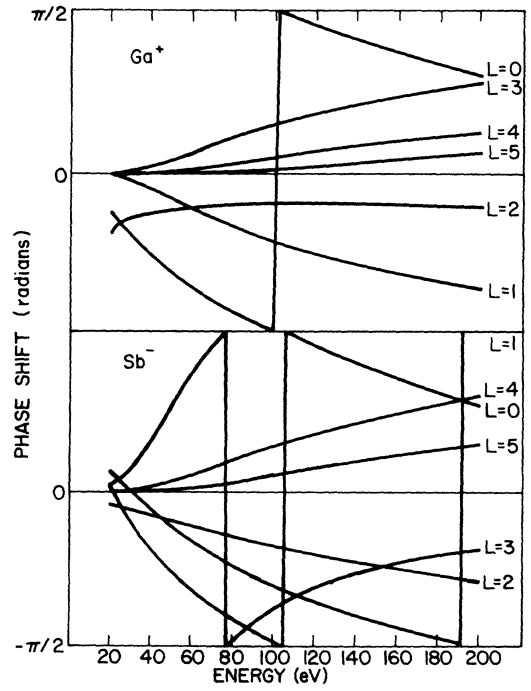

FIG. 2. Phase shifts for the Ga^+ and Sb^- species resulting from relativistic Hara exchange. Since the exchange depends on the energy of the incident electron, so do the muffin-tin radii and potentials, as described in the text.

The electron-electron interaction is incorporated in to the model via a complex inner potential with a constant real part V_0 and an imaginary part characterized by the inelastic collision mean free path λ_{ee}.[18] We selected V_0 to minimize the x-ray R factor[19] [given by Eqs. (3), (8), (13), (14), and (16) of Ref. 19]. Our major structure searches were performed using $\lambda_{ee}=8$ Å, although we examined the sensitivity of the values of the R factors to the value of λ_{ee}.

The consequences of thermal lattice vibrations are neglected in the structure search reported herein, because previous studies of GaAs(110) (Ref. 17) and GaP(110) (Ref. 12) revealed that incorporation of bulk lattice vibrations into the model do not effect the results of the structure analysis. These consequences are not expected to be important in the analysis of ELEED intensity data taken with a spot photometer at temperatures well below the Debye temperature[17,18] which in the case of GaSb is approximately 200 K.[20]

IV. STRUCTURE ANALYSIS

Our analysis of the ELEED intensity data to extract the surface atomic geometry of GaSb(110) proceeded in a fashion analogous to that utilized previously for GaP(110) (Ref. 12) and CdTe(110) (Ref. 21). First, ELEED intensities were calculated for the unreconstructed geometry and for the geometries found for the (110) surfaces of other zinc-blende structure compound semiconductors[9] (suitably scaled to remove the effects of changes in the bulk lattice constant). Then these were compared with the measured intensities and the quality of the description thereof was assessed by both visual and R-factor methods. The x-ray R factor R_x was adopted as the appropriate figure of merit because, as described in detail elsewhere,[12,21] it provides the most reliable index of the quality of the fit of two intensity profiles taken using our techniques (Sec. II). Earlier sensitivity analyses established that for a fixed set of values of the nonstructural model parameters, changes of R_x by 0.02 or greater are significant in comparing one structure to another and increases by 0.04 or more suffice to eliminate a class of structures completely. Values of $0.2 \leq R_x \leq 0.3$ correspond to acceptable but probably not optimal descriptions of the data whereas structures for which $R_x > 0.3$ are unacceptable. (The best struc-

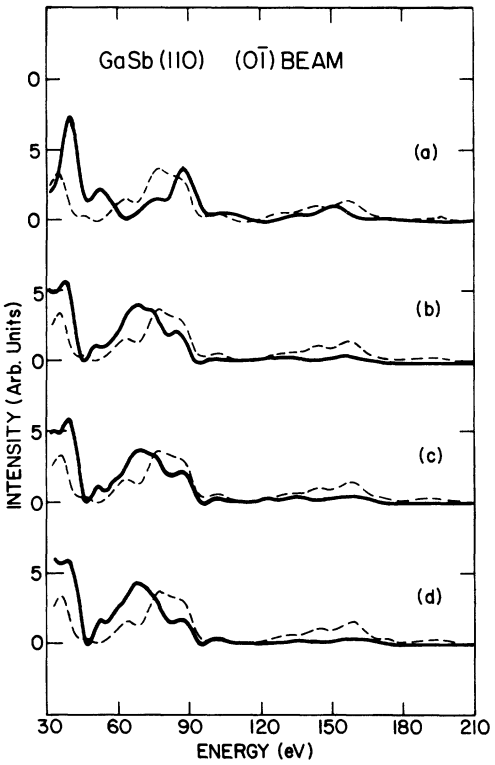

FIG. 3. Comparison of calculated (solid lines) and measured (dashed lines) intensities of electrons normally incident on GaSb(110) diffracted into (0$\bar{1}$) beam. Panel (a): Calculated intensities for the unreconstructed surface structure as specified in panel (a) of Table I, evaluated for a rigid lattice. Panel (b): Calculated intensities for the structure that minimizes the x-ray R factor as specified in panel (b) of Table I, evaluated for a rigid lattice. Panel (c): Calculated intensities for the same structure as panel (b) but with a reduced relaxation parallel to the surface of the Sb in the top layer as specified in panel (c) of Table I. Panel (d): Calculated intensities for the same structure as panel (b) but with a 0.1-Å shear in the second layer as specified in panel (d) of Table I.

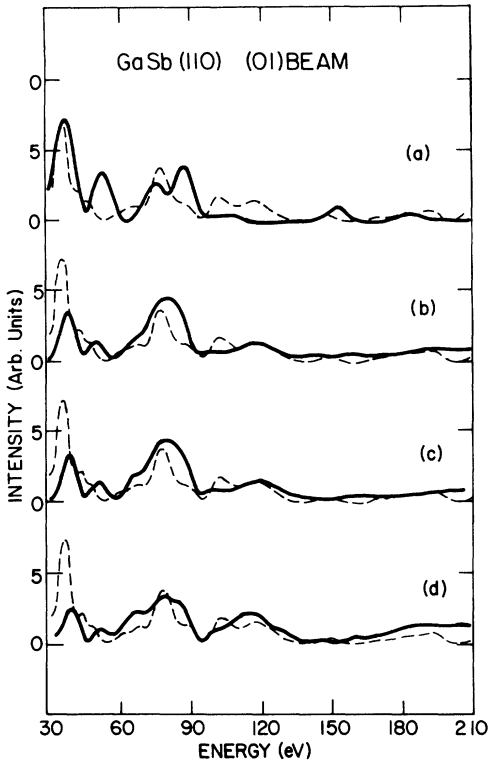

FIG. 4. Same as Fig. 3 for the (01) beam.

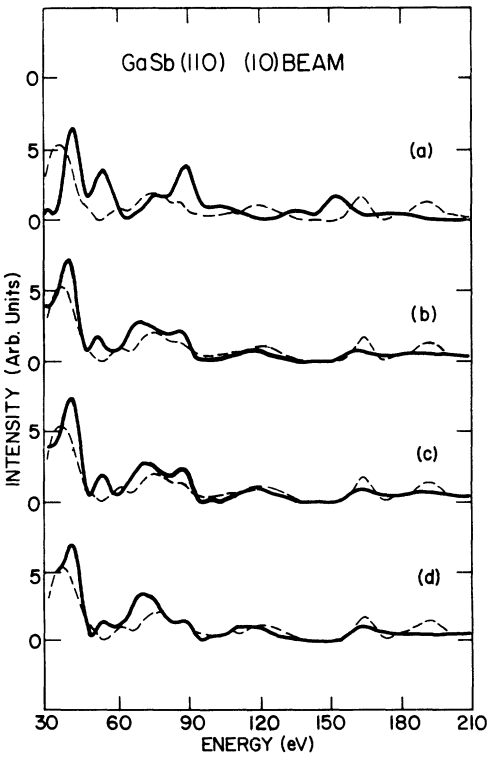

FIG. 5. Same as Fig. 3 for the (10) beam.

tures achieved to date yield $0.14 \leq R_x \leq 0.20$.) This test immediately eliminated the unreconstructed surface ($R_x = 0.38$) and the InP structure[22] ($R_x = 0.31$), and discriminated against the GaAs-InSb-CdTe structure[17,20,23] ($R_x = 0.28$) and the ZnTe structure[14] ($R_x = 0.26$). The unreconstructed atomic geometry is specified in panel (a) of Table I. The comparisons between the calculated and measured ELEED intensities are shown in panels (a) Figs. 3–11 for the strong [(0$\bar{1}$), (01), (10), (11), (02), (1$\bar{1}$), and (0$\bar{2}$)] beams, one medium [(12)] beam and one weak [(2$\bar{1}$)] beam. These figures are presented in order of the decreasing intensities of the beams [e.g., the (0$\bar{1}$) is stronger than the (01), etc.]. It is evident from the

TABLE I. Candidate structures for the surface atomic geometry of GaSb(110). The structural symbols Δ and d are defined in Fig. 1. The angle between the actual plane of the uppermost chain of Ga and Sb and the plane of the truncated bulk surface is designated by ω_1. The inner potential symbol V_0, as well as the R factors R_x, are defined in the text. $\lambda_{ee}=8$ Å for all the calculated R factors in the table.

Structure	Layer	Sb (Å)	Ga (Å)	$\Delta_{1\perp}$ (Å)	$\Delta_{2,1\perp}$ (Å)	$d_{12,1\perp}$ (Å)	$d_{23,1\perp}$ (Å)	Δ_{1y} (Å)	$d_{12,y}$ (Å)	ω_1 deg	Ga_1-Sb_1 % bond-length change	Ga_1-Sb_2 % bond-length change	Sb_1-Ga_2 % bond-length change	V_0 (eV)	λ_{ee} (Å)	R_x
(a)																
Unreconstructed	1	0	0	0	0	2.163	2.163	4.588	3.059	0	0	0	0	12	8	0.38
(b)																
Best fit	1	↑0.22	↓0.55	0.77	0	1.615	2.163	4.793	3.629	30.00	0	−0.03	0	10	8	0.24
(c)																
Reduced Sb relaxation	1	↑0.22	↓0.55	0.77	0	1.615	2.163	4.915	3.629	30.00	−2.21	−0.03	2.12	9	8	0.25
(d)																
Second-layer shear	1	↑0.22	↓0.55	0.77	−0.10	1.565	2.213	4.793	3.629	30.00	0	1.13	−1.68	9	8	0.27
	2	↓0.05	↑0.05													

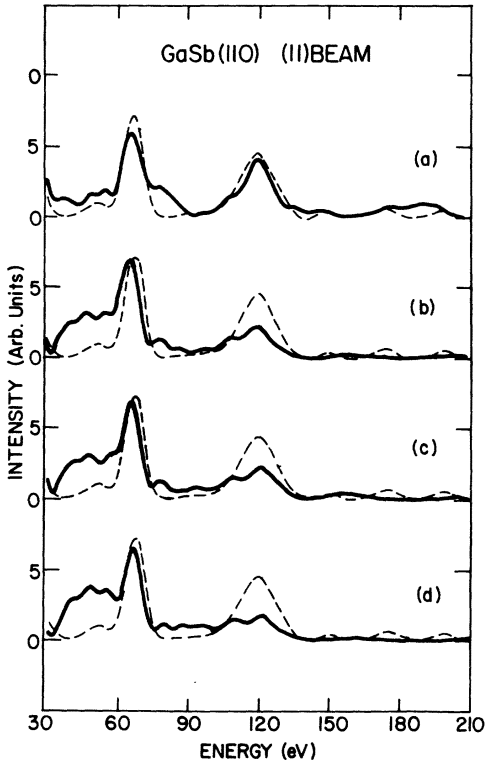

FIG. 6. Same as Fig. 3 for the (11) beam.

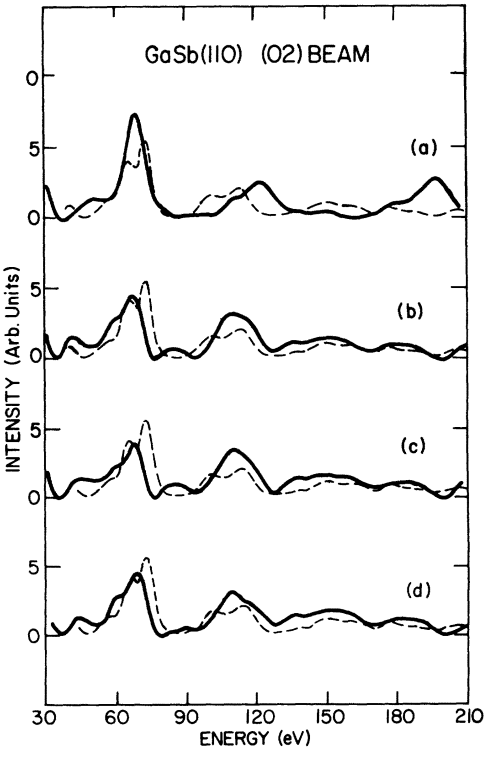

FIG. 7. Same as Fig. 3 for the (02) beam.

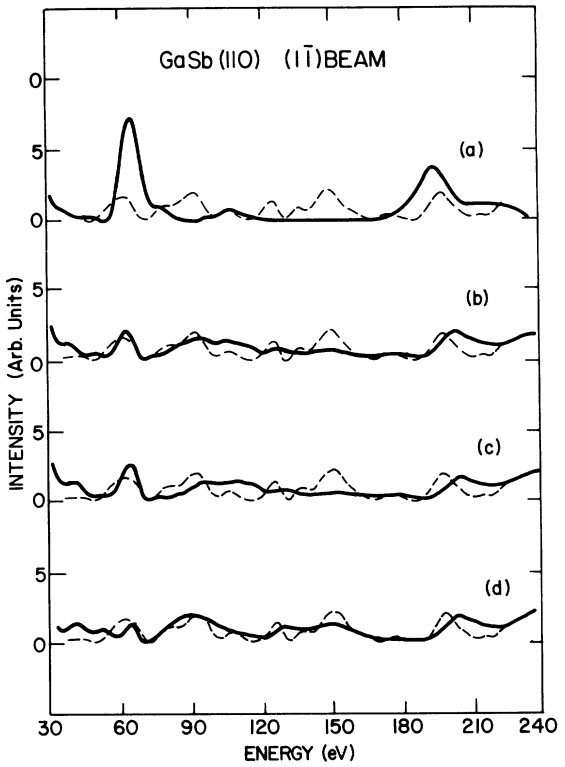

FIG. 8. Same as Fig. 3 for the (1$\bar{1}$) beam.

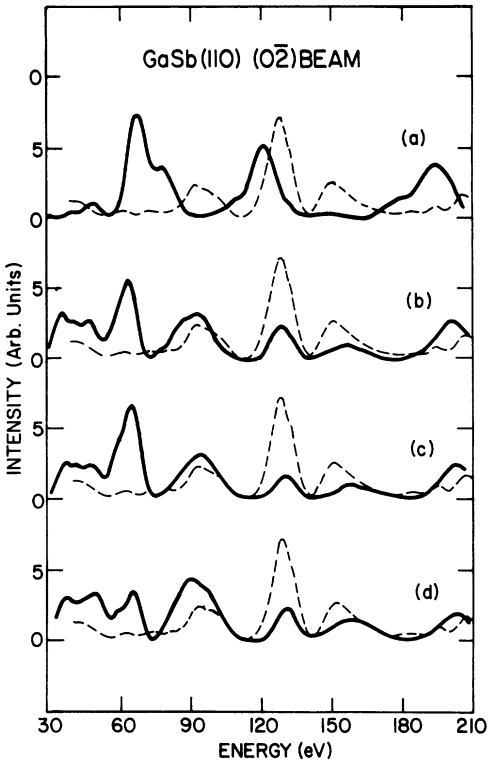

FIG. 9. Same as Fig. 3 for the (0$\bar{2}$) beam.

figures that the unreconstructed geometry provides a poor description of many beams and hence may be eliminated as an acceptable structure for GaSb(110).

Following this preliminary analysis, a systematic search of reconstructions characterized by bond-length–conserving rotations of the top layer was performed. The x-ray R factor exhibits two minima as a function of the angle ω_1 (see Table I), one at $\omega_1=10°$ for which $R_{x,\min}=0.28$ and one at $\omega_1=30°$ for which $R_{x,\min}=0.24$. The latter structure is specified in panel (b) of Table I and the calculated intensities are shown in panels (b) of Figs. 3–11. Increasing λ_{ee} to 10 Å decreased the $\omega_1=30°$ minimum to $R_{x,\min}=0.23$. The $\omega_1=30°$ minimum is an absolute minimum in R_x. Adjustment of the top-layer spacing revealed that expansions of ± 0.1 Å increased R_x by 0.06, well outside $\Delta R_x=0.04$ bounds for absolute discrimination against a structure. Similarly, introduction of a second-layer distortion perpendicular to the surface increased R_x by 0.03, thereby revealing that an undistorted second layer is clearly preferred by the minimum-R_x criterion, although the description of certain beams (e.g., the (01) and (1$\bar{1}$) beams) is improved by such relaxations as may be seen from inspection of panels (d) of Figs. 3–11. Finally, in order to compare the

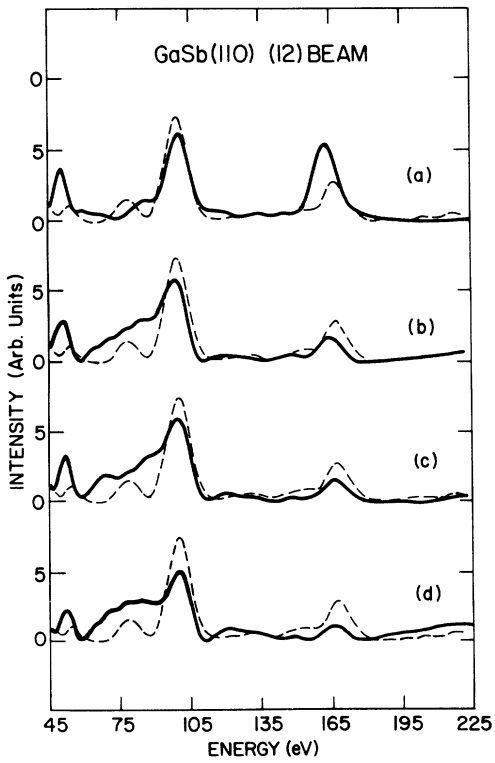

FIG. 10. Same as Fig. 3 for the (12) beam.

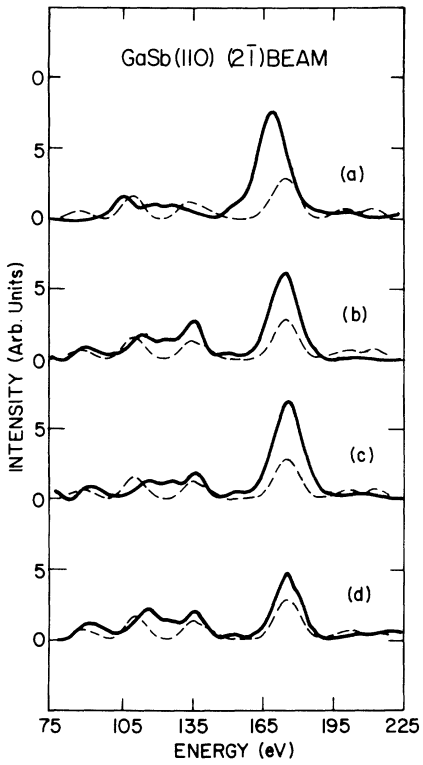

FIG. 11. Same as Fig. 3 for the (2$\bar{1}$) beam.

GaSb(110) structure explicitly with the ZnTe(110) structure, we examined a class of structures in which the relaxation of the Sb parallel to the surface was reduced relative to the $\omega_1=30°$ bond-rotated structure. Again an absolute minimum in R_x is associated with the bond-rotated structure, although in this case the minimum is rather flat so that the position of the Sb along the y axis in Fig. 1 is uncertain to within about ± 0.2 Å. The effects of reducing the Sb relaxation in analogy with the structure found earlier for ZnTe (Ref. 14) are indicated for the structure given in panel (c) of Table I by the calculated intensities shown in panels (c) of Figs. 3–11. The variations in the x-ray R factor associated with these four surface-structure parameters are shown in Fig. 12.

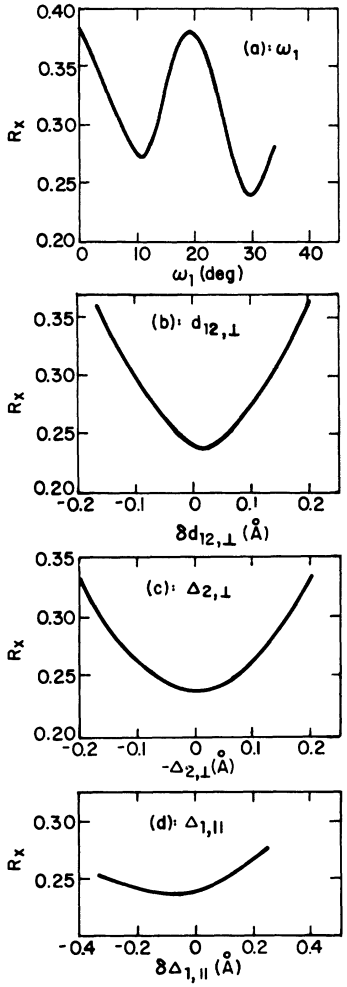

FIG. 12. Values of the x-ray R factors associated with systematic variations of the parameters characteristic of the surface reconstruction of GaSb(110). Panel (a): Variations of ω_1 for a bond-length–conserving top-layer rotation. Panel (b): Variations of the spacing between the top layer and the layer beneath relative to its value for an $\omega_1=30°$ bond-length–conserving, top-layer rotation alone. Panel (c): Variations in the second-layer shear relative to an $\omega_1=30°$ top-layer rotation. Panel (d): Variations in the position of the top layer Sb parallel to the y axis (see Fig. 1) relative to its value for an $\omega_1=30°$ top-layer rotation.

V. SUMMARY AND DISCUSSION

The ELEED intensity analysis reported in Sec. IV reveals that a simple bond-length–conserving top-layer rotation characterized by $\omega_1=(30\pm 2)°$ yields the best description of the intensities measured at $T=125$ K from GaSb(110). This structure corresponds to an absolute minimum in the x-ray R factor and also affords a quite acceptable description of the relative intensities of the various beams. It is significant that the atomic displacements normal to the surface for this structure are identical to those found earlier[14] for ZnTe(110). GaSb is isoelectronic with ZnTe, but its bonding is much more covalent (e.g., the spectroscopic ionicities[7] of GaSb and ZnTe are 0.26 and 0.55, respectively). Therefore we have another example, similar to that afforded by the isoelectronic CdTe-InSb pair,[21,23] in which two materials of widely varying spectroscopic ionicities ex-

hibit quite similar atomic geometries on their (110) surfaces.

The relationship between the properties of semiconductor interfaces and the nature of the bonding in the bulk semiconductors is a venerable and controversial topic.[15] Recent interest in the subject was stimulated by the proposal in 1969 by Kurtin, McGill, and Mead[24] of a correlation between the heights of rectifying Schottky barriers on binary compound semiconductors and the difference in ionicities of the two elements which comprise the binary semiconductor. In particular, it was suggested[24] that a transition between "covalent" and "ionic" interface properties occurs at a difference in ionicity of $\Delta X \simeq 0.7$, determined using the "Pauling" scale.[6] This proposal stimulated an enormous volume of subsequent work, as may be verified by inspection of recent reviews of Schottky barrier formation.[6,25] An expression of this proposal in terms of the dielectric function of the bulk semiconductor (and hence of the spectroscopic ionicity[7]) was given by Phillips.[2] His analysis was subsequently extended (and corrected) by Barrera and Duke,[26] and shown to be incompatible with measured values of the barrier heights.

The idea persisted, however, that a transition from covalent to ionic interface behavior might occur within the tetrahedrally coordinated compound semiconductors. Early LEED studies of the atomic geometries of GaAs(110) and ZnO($10\bar{1}0$) were compatible with this concept because they revealed quite different reconstructions for the bulk geometries for these two surfaces.[27] As more compound semiconductor surface structures become available, they initially seemed compatible[15] with a transition in the character of the surface structures of the (charge-neutral) cleavage faces at a spectroscopic ionicity of $f_i \simeq 0.5$. The subsequent determination of the structure of CdTe(110) revealed, however, that the spectroscopic ionicity could not be used as a suitable scale to correlate with the atomic geometries of zinc-blende structure compound semiconductors, although the ionicity scale used by Kurtin, McGill, and Mead did correlate satisfactorily with all of the surface geometries at that time.[21]

The important role of the atomic geometry of GaSb(110) in establishing the nature of correlations of surface structure with indices of the nature of the chemical bond in bulk compound semicondctors can now be appreciated. The spectroscopic ionicity of GaSb is $f_i = 0.26$ (Ref. 7) whereas the difference in Pauling electronegativities of Sb and Ga is 0.3 (Ref. 6, p. 93). Both values lie comfortably on the covalent side of the critical ionicity [$f_{ic} \simeq 0.5$ (Ref. 15), $\Delta X_c \simeq 0.7$ (Ref. 24)] characteristic of the proposed transition in interface properties. Yet there is no evidence in GaSb(110) for the multilayer reconstruction characteristic of the (110) surface of GaAs,[17] InSb,[23] and CdTe,[21] i.e., the reconstruction previously associated[15] with the covalent limit of zinc-blende (110) surface structures. Thus, the analysis of low-temperature ELEED intensities from GaSb(110), in concert with the results for CdTe(110) (Ref. 21), establish that the multilayer character of the reconstruction of zinc-blende (110) surfaces cannot be correlated simply with either the spectroscopic[7] or Pauling[6,24] ionicities. This result cannot be inferred from the analysis of room temperature ELEED data [as done, e.g., for GaP(110) in Ref. 12] because the energy gained by reconstruction of the second and deeper layers is comparable to thermal energies at room temperature.[28] The only correlation which we have been able to identify between the chemical species and the occurrence of strong ELEED evidence for second-layer reconstructions is that both elements of the binary compound semiconductor must lie in the same row of the Periodic Table.

In summary, analysis of ELEED intensities from GaSb(110) at $T = 125$ K reveals a simple top-layer bond-rotated reconstruction corresponding to $\omega_1 = (30 \pm 2)°$. The accuracy of the atomic displacements normal to the surface is $\Delta d_\perp \simeq 0.05$ Å whereas that of displacements parallel to the surface is $\Delta d_{||} \simeq 0.2$ Å. This structure is similar but not identical to that hypothesized for use in recent calculations of electronic states at GaSb(110) surfaces.[29] The absence of second-layer relaxations eliminates the Pauling[6,24] as well as spectroscopic[7] ionicity scale as a suitable index of the character of the chemical bond to correlate with ELEED evidence for the occurrence of multilayer as opposed to single-layer low-temperature reconstructions of the cleavage faces of tetrahedrally coordinated compound semiconductors.

ACKNOWLEDGMENTS

The authors are indebted to Dr. P. Skeath of Stanford University for the GaSb crystal, to Ms. L. J. Kennedy for assistance, to Dr. W. K. Ford for useful conversations on the construction of the relativistic Hara potentials, and to Dr. M. D. Tabak for his generous support of this work.

[1]C. A. Mead, Solid State Electron. 9, 1023 (1966).
[2]J. C. Phillips, Solid State Commun. 12, 861 (1973).
[3]C. B. Duke, Mater. Sci. Eng. 25, 13 (1976).
[4]W. E. Spicer, I. Lindau, P. Skeath, and C. Y. Su, J. Vac. Sci. Technol. 17, 1019 (1980).
[5]L. J. Brillson, J. Vac. Sci. Technol. 20, 652 (1982).
[6]L. Pauling, *The Nature of the Chemical Bond,* 3rd ed. (Cornell University Press, Ithaca, 1973).
[7]J. C. Phillips, Rev. Mod. Phys. 42, 317 (1970).
[8]*Structure and Bonding in Crystals* edited by M. O'Keeffe and A. Navrotsky (Academic, New York, 1981), Vol. I.
[9]C. B. Duke, Adv. Ceram. 4, 1 (1983).
[10]R.W.G. Wyckoff, *Crystal Structures* (Wiley, New York, 1963), Vol. I, p. 108.
[11]C. B. Duke, R. J. Meyer, A. Paton, A. Kahn, J. Carelli, and J. L. Yeh, J. Vac. Sci. Technol. 18, 866 (1981).
[12]C. B. Duke, A. Paton, W. K. Ford, A. Kahn, and J. Carelli, Phys. Rev. B 24, 562 (1981).
[13]B. W. Lee, R. K. Ni, N. Masud, X. R. Wang, D. C. Wang, and M. Rowe, J. Vac. Sci. Technol. 19, 294 (1981).
[14]R. J. Meyer, C. B. Duke, A. Paton, E. So, J. L. Yeh, A. Kahn, and P. Mark, Phys. Rev. B 22, 2875 (1980).
[15]C. B. Duke, R. J. Meyer, and P. Mark, J. Vac. Sci. Technol. 17, 971 (1980).
[16]W. K. Ford, C. B. Duke, and A. Paton, Surf. Sci. 115, 195 (1982).
[17]R. J. Meyer, C. B. Duke, A. Paton, A. Kahn, E. So, J. L. Yeh, and P. Mark, Phys. Rev. B 19, 5194 (1979).
[18]C. B. Duke, Adv. Chem. Phys. 27, 1 (1974); in *Dynamic Aspects of Surface Physics, Proceedings of the International School of Physics, "Enrico Fermi," Course LVIII,* edited by F. O. Goodman (Editrice Compositori, Bologna, 1974), pp. 99–173.
[19]E. Zanazzi and F. Jona, Surf. Sci. 62, 61 (1977).
[20]V. T. Bublik and S. S. Gorelik, Krist. Tech. 12, 859 (1977).
[21]C. B. Duke, A. Paton, W. K. Ford, A. Kahn, and G. Scott, Phys. Rev. B 24, 3310 (1981).
[22]R. J. Meyer, C. B. Duke, A. Paton, J. C. Tsang, J. L. Yeh, A. Kahn, and P. Mark, Phys. Rev. B 22, 6171 (1980).
[23]R. J. Meyer, C. B. Duke, A. Paton, J. L. Yeh, J. C. Tsang, A. Kahn, and P. Mark, Phys. Rev. B 21, 4740 (1980).
[24]S. Kurtin, T. C. McGill, and C. A. Mead, Phys. Rev. Lett. 22, 1433 (1969).
[25]L. J. Brillson, Surf. Sci. Reps. 2, 123 (1982).
[26]R. G. Barrera and C. B. Duke, Phys. Rev. B 13, 4477 (1976).
[27]C. B. Duke, A. R. Lubinsky, B. W. Lee, and P. Mark, J. Vac. Sci. Technol. 13, 761 (1976).
[28]D. J. Chadi, Phys. Rev. B 19, 2074 (1979).
[29]R. E. Allen, J. D. Dow, and H. P. Hjalmarson, Solid State Commun. 41, 419 (1982).